

Discovery of a Proneurogenic, Neuroprotective Chemical

Andrew A. Pieper,^{1,2,*} Shanhai Xie,¹ Emanuela Capota,² Sandi Jo Estill,¹ Jeannie Zhong,² Jeffrey M. Long,¹ Ginger L. Becker,² Paula Huntington,² Shauna E. Goldman,² Ching-Han Shen,¹ Maria Capota,² Jeremiah K. Britt,² Tiina Kotti,¹ Kerstin Ure,³ Daniel J. Brat,⁴ Noelle S. Williams,¹ Karen S. MacMillan,¹ Jacinth Naidoo,¹ Lisa Melito,¹ Jenny Hsieh,³ Jef De Brabander,¹ Joseph M. Ready,¹ and Steven L. McKnight^{1,*}

¹Department of Biochemistry

²Department of Psychiatry

³Department of Molecular Biology

UT Southwestern Medical Center, 5323 Harry Hines Boulevard, Dallas, TX 75390-9152, USA

⁴Department of Pathology and Laboratory Medicine, Emory University School of Medicine, Atlanta, GA 30332, USA

*Correspondence: andrew.pieper@utsouthwestern.edu (A.A.P.), steven.mcknight@utsouthwestern.edu (S.L.M.)

DOI 10.1016/j.cell.2010.06.018

SUMMARY

An *in vivo* screen was performed in search of chemicals capable of enhancing neuron formation in the hippocampus of adult mice. Eight of 1000 small molecules tested enhanced neuron formation in the subgranular zone of the dentate gyrus. Among these was an aminopropyl carbazole, designated P7C3, endowed with favorable pharmacological properties. *In vivo* studies gave evidence that P7C3 exerts its proneurogenic activity by protecting newborn neurons from apoptosis. Mice missing the gene encoding neuronal PAS domain protein 3 (NPAS3) are devoid of hippocampal neurogenesis and display malformation and electrophysiological dysfunction of the dentate gyrus. Prolonged administration of P7C3 to *npas3*^{-/-} mice corrected these deficits by normalizing levels of apoptosis of newborn hippocampal neurons. Prolonged administration of P7C3 to aged rats also enhanced neurogenesis in the dentate gyrus, impeded neuron death, and preserved cognitive capacity as a function of terminal aging.

INTRODUCTION

Inspirational work led by Fernando Nottebohm has proven that the adult vertebrate brain fosters the birth and functional incorporation of newly formed neurons (Paton and Nottebohm, 1984). Nottebohm's studies on neuron birth as a prerequisite for avian song learning validated earlier claims of adult neurogenesis by Joseph Altman in the 1960s. Altman challenged the prevailing neuroscience dogma that no new neurons could be added to the adult mammalian brain when he reported autoradiographic evidence of new neuron formation in the hippocampal dentate gyrus, olfactory bulb, and cerebral cortex of adult rats (Altman, 1962; Altman and Das, 1965). It is now accepted that all mammalian species, including humans, harbor

reservoirs of neuronal stem cells in the subgranular zone (SGZ) of the hippocampal dentate gyrus and the subventricular zone (SVZ) (Gross, 2000). Neural stem cells in the SVZ facilitate formation of new neurons that migrate rostrally to the olfactory bulb. Neural stem cells in the SGZ produce neurons that integrate locally in the granular layer of the dentate gyrus, a region of the hippocampus that exhibits lifelong structural and functional plasticity.

New neuron formation in the adult mouse brain is influenced by environmental, chemical, and genetic variables, such as environmental enrichment (Kempermann et al., 1997) or voluntary exercise (van Praag et al., 1999). Administration of antidepressant drugs to rodents and humans has also been reported to enhance adult neurogenesis (Schmidt and Duman, 2007; Boldrini et al., 2009). Among many genes reported to impact adult neurogenesis is the gene encoding NPAS3, a central nervous system-specific transcription factor that is associated with learning disability and mental illness (Kamnasaran et al., 2003; Pickard et al., 2005, 2006, 2009; Macintyre et al., 2010).

Npas3^{-/-} mice display behavioral abnormalities (Erbel-Sieler et al., 2004) and a profound loss of adult hippocampal neurogenesis (Pieper et al., 2005). As will be shown, *npas3*^{-/-} mice also display dentate granular cell dysmorphologies and aberrations in synaptic transmission. Here, we report the results of an *in vivo* screen for small molecules capable of restoring hippocampal neurogenesis to *npas3*^{-/-} mice.

RESULTS

Computational methods were employed to select 1000 compounds from a library of 200,000 drug-like chemicals with consideration of chemical diversity, complexity, and potential toxicity. Compounds were randomly pooled into groups of ten and administered by intracerebroventricular (ICV) injection at a constant rate over 7 days into the left lateral ventricle of living mice via osmotic minipumps. Compounds were administered at a concentration of 10 μ M each, making total solute concentration 100 μ M. Although it is difficult to predict the final brain concentration of each compound over the 7 day infusion

period, we designed our screen with a logical consideration of this variable. At 10 μM concentration, it is reasonable to estimate that compounds were administered at low-micromolar to mid-nanomolar concentrations (Extended Experimental Procedures).

During compound infusion, animals received intraperitoneal (IP) injection daily with the thymidine analog bromodeoxyuridine (BrdU, 50 mg/kg) to score birth and survival of proliferating hippocampal neural precursor cells. Because social interaction and voluntary exercise stimulate hippocampal neurogenesis, mice were housed individually without access to running wheels starting 1 week prior to screening in order to ensure a low baseline level of neurogenesis. After 1 week of compound administration, BrdU immunohistochemistry was used to quantify neurogenesis in the SGZ of the brain hemisphere contralateral to the side of infusion. Every fifth section throughout the rostral-caudal extent of the hippocampus was analyzed, and the number of BrdU+ cells was normalized against the volume of the dentate gyrus.

Because we considered both increased proliferation and survival of newborn neurons to be important screening parameters, we conducted our screen over 7 days in order to detect molecules that might augment either process. This was based on pulse-chase experiments with a single injection of BrdU, under identical conditions to our screen, which revealed that 40% of newborn cells in the SGZ die within the first 5 days after their birth (Figure S1A available online). ICV infusions of either fibroblast growth factor 2 (FGF-2) or artificial cerebral spinal fluid (aCSF) were employed as positive and negative controls. There was no difference in the number of BrdU+ cells in the SGZ between mice subjected to surgical pump implantation and infusion with aCSF and mice having had no surgery (Figure S1B). This confirmed the validity of our *in vivo* approach to assess the ability of ICV-infused compounds to enhance hippocampal neurogenesis in the brain hemisphere contralateral to that of compound infusion.

We reasoned that it was important that neurogenesis triggered by any compound be localized to the exact region of the brain known to produce new neurons at an enhanced level in response to healthy conditions such as wheel running, environmental enrichment, or social interaction. We thus focused solely on compound pools that stimulated BrdU incorporation in the SGZ of the dentate gyrus (Figure S1C).

Each pool was tested on two mice, and ten pools were found to enhance dentate gyrus-specific neurogenesis as much as FGF-2 (Figure 1A). Each pool that scored positive was re-evaluated in two additional mice and verified to exert a proneurogenic effect with statistical significance (Figure S1D). In order to identify single, proneurogenic compounds, we broke down positive pools into their component molecules, each of which was infused individually at two concentrations (10 μM and 100 μM) in two mice per concentration. Figure 1B shows the results of breakdown assays on pool #7, wherein it was discovered that neurogenesis was selectively stimulated by one of the constituent chemicals of the pool (compound #3), with the remaining chemicals in the pool demonstrating no effect. We have designated this compound as P7C3 (pool #7, compound #3).

Of the ten positive pools, eight yielded a single proneurogenic compound (Table S1). Pools 14 and 69 failed to reveal activity in

a single species. The activity of these pools may have been artifactually spurious or may have been generated by the combined activity of two or more compounds. We considered both scenarios sufficiently problematic such that we disregarded these pools and focused exclusively on individually efficacious molecules. To ensure validity of the eight individually efficacious molecules, we obtained fresh compounds from the original manufacturer, confirmed purity and molecular weight by liquid chromatography-mass spectrometry (LC-MS), and then assayed each one at 10 μM in three additional mice. All eight resupplied compounds demonstrated SGZ-specific proneurogenic activity (Figure S1E).

Among the eight proneurogenic compounds, *in silico* prediction of absorption, distribution, metabolism, and excretion (ADME) characteristics suggested that P7C3 held the highest potential for favorable pharmacological properties. Fortuitously, P7C3 could be formulated for intravenous (IV), oral, and IP delivery, allowing determination of half-life, rate of clearance, bioavailability, and blood brain barrier penetration. Noncompartmental pharmacokinetic analysis of P7C3 in plasma and whole-brain tissue was undertaken after single IV, IP, and oral gavage administrations. P7C3 was 32% orally bioavailable, readily able to cross the blood-brain barrier (AUC brain: AUC plasma ratio of 3.7 for oral delivery), and endowed with a plasma terminal half life of 6.7 hr after IP delivery. These favorable properties facilitated a dose-response experiment wherein daily oral administration of P7C3 for 7 days to adult mice was monitored for brain levels of the chemical and proneurogenic efficacy (Figure 1C). Maximal, proneurogenic efficacy was observed at oral doses of 5 mg/kg and above, and graded reductions in efficacy were observed at doses of 2.5 and 1 mg/kg. LC-MS analysis of brain levels of P7C3 in the dose ranges of 1 and 2.5 mg/kg revealed corresponding compound concentrations of 213 nM (101 ng/g brain tissue) and 1.13 μM (534 ng/g brain tissue) 5 hr after dosing.

Functional Studies of Chemical Variants of P7C3

To further evaluate the properties of P7C3, we conducted an *in vivo* structure activity relationship (SAR) study using 37 chemical derivatives of the compound for assessment of proneurogenic activity as performed in the original screen (Figure 2A). One variant showed activity enhancement, while roughly 15% retained proneurogenic activity indistinguishable from the parent compound. A handful of compounds yielded partially diminished activity, and the majority were inactive.

The single derivative of P7C3 exhibiting enhanced activity (P7C3A20) replaced the hydroxyl group at the chiral center of the linker with fluorine. Two other variants that have been employed as controls in later experiments were inactive. One of these (P7C3A29) replaced the aniline moiety with a pyrazole. The other (P7C3A35) lengthened the linker connecting the tricyclic carbazole to the aniline ring by a CH₂ unit (Figure 2B).

Among compounds retaining activity equivalent to the parent molecule was a variant (P7C3-OMe) in which the aniline ring of P7C3 was substituted by an anisidine. This variant lent itself to preparation of *R*- and *S*-enantiomers around its single chiral center (Figure 2B). The two enantiomers of P7C3-OMe were synthesized, separated, and evaluated in the *in vivo*

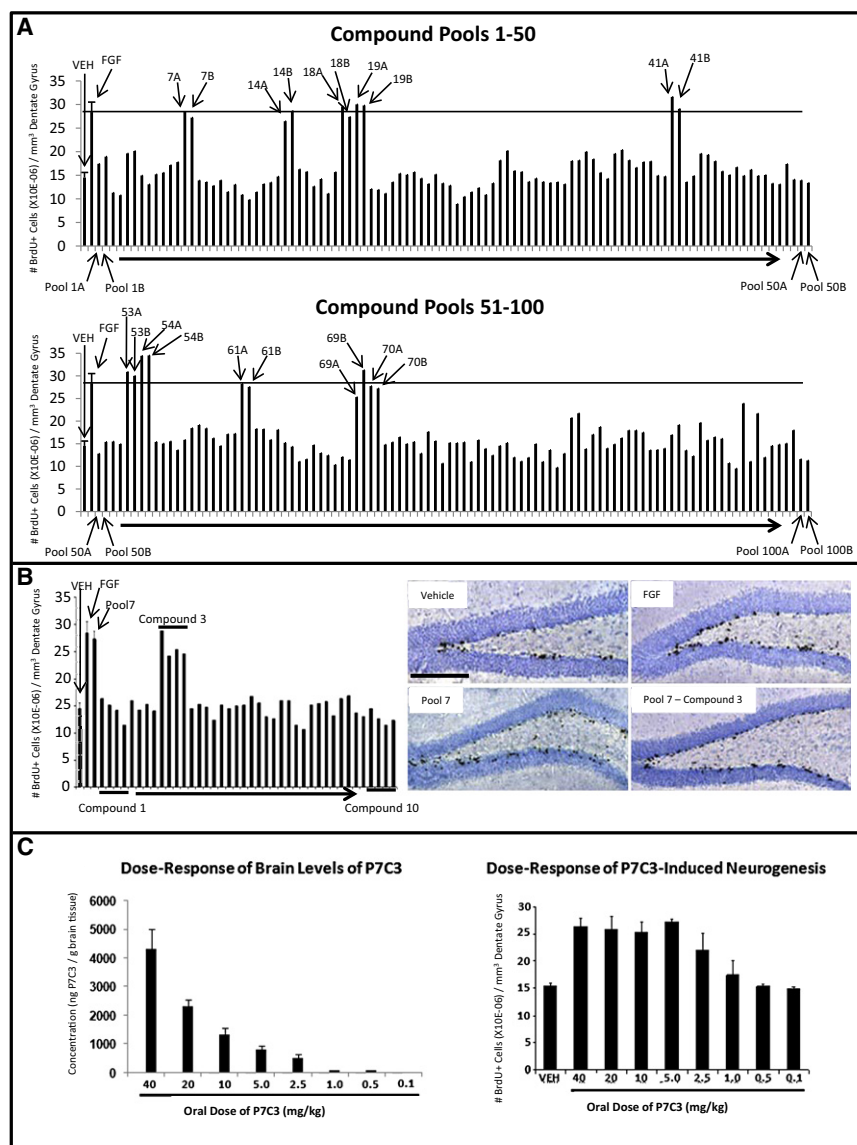


Figure 1. In Vivo Screen for Proneurogenic Molecules

(A) The total number of BrdU+ cells in the SGZ doubled after 7 day infusion with FGF-2 relative to vehicle. Each pool of ten compounds was tested for proneurogenic efficacy in two mice, and ten pools displayed efficacy comparable to FGF-2 infusion. The majority of pools displayed no effect.

(B) In vivo evaluation in four mice each of the ten individual compounds in pool #7 revealed exclusive activity for compound #3. Immunohistochemically visualized BrdU incorporation in the SGZ is notably greater in animals infused with either pool #7 or compound #3 from pool #7 relative to vehicle-infused animals. All micrographs were taken at the same magnification. (The scale bar represents 200 μ m.)

(C) P7C3 concentration in mouse brain tissue correlated with oral dosing. Proneurogenic efficacy of P7C3 was roughly double that of vehicle at doses ranging from 5 to 40 mg/kg. At decreasing dosage of P7C3 the amount of neurogenesis decreased accordingly, until reaching levels no greater than vehicle at compound doses below 1.0 mg/kg.

In all graphs, data are expressed as mean \pm standard error of the mean (SEM). See also Figure S1 and Table S1.

neurogenesis attributable to increased levels of cell proliferation? Or, instead, might it be that P7C3 enhances neurogenesis by protecting newborn neurons from cell death during the month-long differentiation pathway taken between their birth and eventual incorporation into the dentate gyrus granular layer as properly wired neurons?

To address the first question, we stained brain tissue from animals exposed to orally administered P7C3 for 30 days for doublecortin (DCX), a microtu-

bule-associated protein that serves as a marker of neurogenesis by virtue of transient expression in newly formed neurons between the timing of their birth and final maturation (Brown et al., 2003). As shown in Figure 3A, the relative abundance of DCX+ neurons increased dramatically with prolonged administration of P7C3. Prolonged exposure of mice to P7C3 further resulted in generation of BrdU+ cells coexpressing the NeuN and Prox1 markers of mature neurons (Figure S2A). By contrast, prolonged P7C3 administration did not affect the abundance of hippocampal astrocytes or oligodendrocytes (Figure S2B). In combination, these immunohistochemical assays confirm the fact that P7C3 enhances neuron formation in the hippocampus of adult mice.

neurogenesis assay, and the *R*-enantiomer was noted to retain the vast majority of proneurogenic activity. Figure 2B shows the results of dose-response studies wherein the activity of the parent compound (P7C3) was compared with the activities of the hydroxyl-to-fluorine variant (P7C3A20), the two enantiomers of P7C3-OMe, and the two inactive variants (P7C3A29 and P7C3A35). These dose-response assays confirmed that (1) P7C3A20 is superior in proneurogenic efficacy to the parent compound, (2) the *R*-enantiomer of P7C3-OMe is far more active than the *S*-enantiomer, and (3) P7C3A29 and P7C3A35 are inactive.

P7C3 Enhances Survival of Newborn Neurons

Access to P7C3, an easily administered proneurogenic compound, allowed prosecution of two questions. First, what sorts of cells are produced after P7C3 enhances BrdU incorporation in the SGZ? Second, is P7C3-mediated enhancement of

neurogenesis attributable to increased levels of cell proliferation? Or, instead, might it be that P7C3 enhances neurogenesis by protecting newborn neurons from cell death during the month-long differentiation pathway taken between their birth and eventual incorporation into the dentate gyrus granular layer as properly wired neurons?

To address the first question, we stained brain tissue from animals exposed to orally administered P7C3 for 30 days for doublecortin (DCX), a microtu-

bule-associated protein that serves as a marker of neurogenesis by virtue of transient expression in newly formed neurons between the timing of their birth and final maturation (Brown et al., 2003). As shown in Figure 3A, the relative abundance of DCX+ neurons increased dramatically with prolonged administration of P7C3. Prolonged exposure of mice to P7C3 further resulted in generation of BrdU+ cells coexpressing the NeuN and Prox1 markers of mature neurons (Figure S2A). By contrast, prolonged P7C3 administration did not affect the abundance of hippocampal astrocytes or oligodendrocytes (Figure S2B). In combination, these immunohistochemical assays confirm the fact that P7C3 enhances neuron formation in the hippocampus of adult mice.

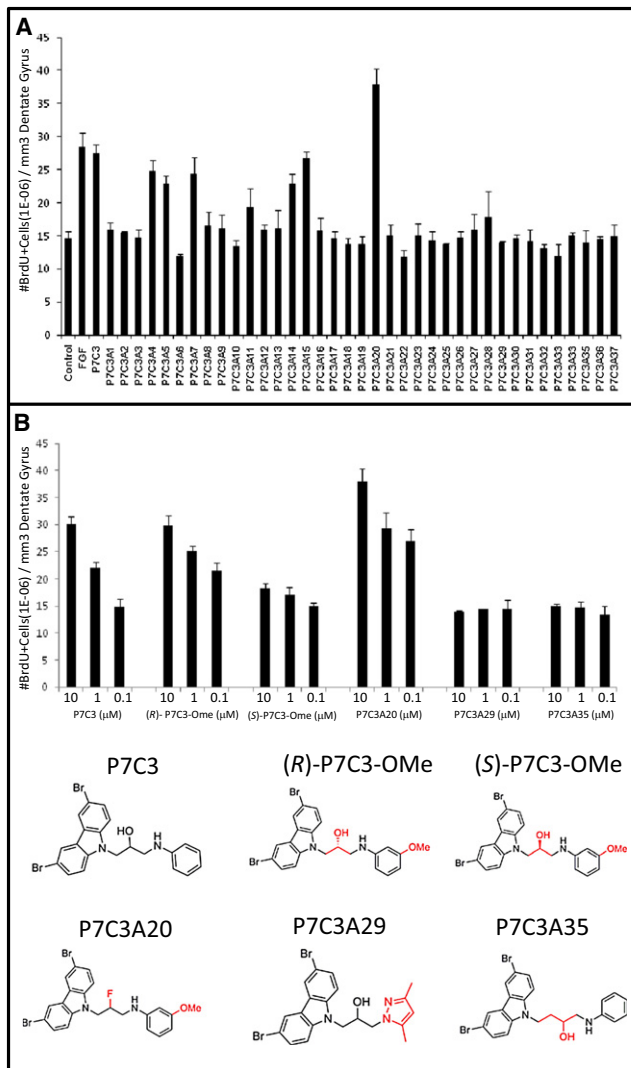


Figure 2. SAR Analysis of Structural Variants of P7C3

(A) An *in vivo* SAR study with 37 analogs of P7C3 showed that some analogs had proneurogenic activity comparable to the parent compound, whereas others had either no activity or activity intermediate between vehicle and FGF controls. A single compound (P7C3A20) showed enhanced efficacy.

(B) Comparison of proneurogenic efficacy of analogs of P7C3 showed that the (*R*)-enantiomer of P7C3-OMe was active, whereas the (*S*)-enantiomer was not. P7C3A20 exhibited enhanced activity, while P7C3A29 and P7C3A35 suffered structural changes that abolished activity.

In all graphs, data are expressed as mean \pm SEM.

(150 mg/kg) via IP injection. Short-term effects on neuron birth were monitored by sacrifice of animals 1 hr after BrdU injection after P7C3 had been administered for 7 days, followed by immunohistochemical detection of BrdU in the SGZ. P7C3 administration did not elevate the level of BrdU+ cells relative to vehicle in this short-term assay (Figure 3B). At the 1 day after BrdU administration time point, both groups still showed no statistically significant differences in the number of BrdU+ cells. By the 5 day time point, at which time 40% of cells born by day 1 normally die (Figure S1A), animals that received P7C3 showed

a statistically significant, 25% increase in BrdU+ cells compared to the vehicle group. This difference progressed with time such that mice that received a daily oral dose of P7C3 for 30 days after the BrdU pulse exhibited a 500% increase in abundance of BrdU+ cells in the dentate gyrus relative to vehicle controls (Figure 3B).

In this longer-term trial, BrdU+ cells were observed both within the SGZ and the granular layer (Figure 3B). We hypothesize that the latter, BrdU+ cells represent mature neurons that have functionally incorporated into the dentate gyrus. Observations supportive of this interpretation will be presented in a subsequent section of this report. In summary, these experiments show that P7C3 enhances the formation of neurons in the mature hippocampus and that its mode of action takes place subsequent to the initiation of neural precursor cell proliferation.

P7C3 Corrects Deficits in the Dentate Gyrus of *npas3*^{-/-} Mice

Npas3^{-/-} mice suffer a clear-cut impairment in adult neurogenesis (Pieper et al., 2005). By evaluating BrdU incorporation in the short-term assay 1 hr after BrdU pulse, it was observed that *npas3*^{-/-} mice have no deficit in the initial proliferation of neural precursor cells in the SGZ (Figure S3A). This is in contrast to our earlier observations of profoundly diminished BrdU labeling in the dentate gyrus of *npas3*^{-/-} mice when BrdU was administered for a longer period of time (12 days) (Pieper et al., 2005). Knowing that NPAS3 is required for proper expression of fibroblast growth factor receptor 1 in the hippocampus (Pieper et al., 2005), it is possible that impediments in growth factor signaling might impair the trophic environment critical for survival of newborn neurons in the dentate gyrus. To test this idea, we compared brain tissue from *npas3*^{-/-} mice with that of wild-type littermates for the presence of cleaved caspase 3 (CCSP3)-positive (apoptotic) cells in the SGZ. A statistically significant, 3-fold increase in CCSP3-positive cells was observed in the dentate gyrus of *npas3*^{-/-} mice (Figure S3A). This enhanced level of apoptosis is likely to account, at least in part, for the nearly complete elimination of adult neurogenesis in *npas3*^{-/-} mice.

In addition to a deficit in adult neurogenesis, *npas3*^{-/-} mice display abnormalities in both the morphology and electrophysiology of dentate gyrus granular neurons. Relative to wild-type animals, Golgi-Cox staining revealed severe attenuation in dendritic branching and spine density of *npas3*^{-/-} dentate gyrus granular neurons (Figure 4A). Significant genotype-specific deficits were also observed by comparing electrophysiologic recordings of excitatory postsynaptic potentials (eEPSP) of *npas3*^{-/-} mice with wild-type littermates (Figure 4B). Such studies revealed aberrant hyperexcitability of synaptic transmission in *npas3*^{-/-} mice both in the outer molecular layer of the dentate gyrus and in the CA1 region of the hippocampus (Figure 4B).

Armed with these genotype- and region-specific deficits in neuron morphology and electrophysiological activity, we set out to test whether prolonged administration of P7C3 might repair either or both deficits in *npas3*^{-/-} mice. We first verified that P7C3 was capable of enhancing hippocampal neurogenesis in *npas3*^{-/-} mice (Figure S3B). Knowing that formation of the dentate gyrus initiates in the mouse embryo around embryonic

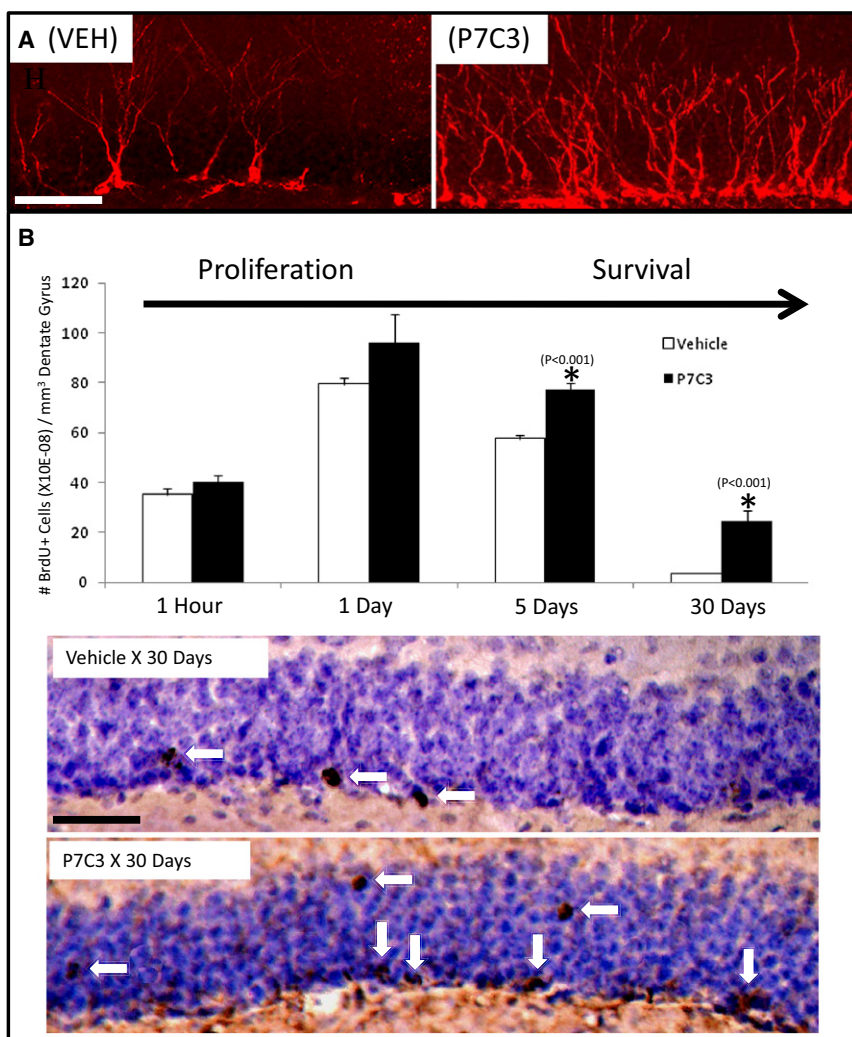


Figure 3. P7C3 Treatment Enhances Production and Survival of Neural Precursor Cells Destined to a Neuronal Fate

(A) Immunohistochemical staining for DCX was increased in newborn neurons in mice that were administered P7C3.

(B) P7C3 enhances hippocampal neurogenesis by promoting survival of newborn neurons without affecting proliferation.

In both (A) and (B), both sets of micrographs were taken at the same magnification (scale bars represent 50 μ m) and are representative of ten sections from each of five mice in each group. Data are expressed as mean \pm SEM. See also Figure S2.

day 14 (Stanfield and Cowan, 1988), we sought to expose animals to P7C3 for as extended a period of time as possible in order to give the compound the best possible chance for success. After oral gavage of pregnant female mice, day 14 embryos were recovered, dissected, and processed by acetonitrile:water extraction so that P7C3 levels could be measured in the embryonic brain. Daily administration of 20 mg/kg of P7C3 to pregnant females yielded appreciable levels of the compound in the brain tissue of developing embryos. It was similarly observed that oral administration of the compound to lactating females led to delivery of P7C3 to the brain tissue of weanling pups. In both cases, LC-MS-based quantitation of P7C3 revealed levels of compound accumulation at or above the 1.35 μ M limit required to support adult neurogenesis (Figure 1C). Finally, it was observed that daily IP administration of P7C3 to weaned pups at 20 mg/kg yielded brain levels of P7C3 at or above the level required to enhance adult neurogenesis.

Female mice heterozygous at the NPAS3 locus were mated to heterozygous males. Two weeks after mating, females were given a daily oral gavage of either 20 mg/kg of P7C3 or vehicle. Dosing was continued throughout the last trimester of

pregnancy, as well as the 3 week post-natal period of lactation. After weaning, pups were given a daily IP dose of either 20 mg/kg P7C3 or vehicle. At about 7 weeks of age, mice were switched to oral gavage of the same dose of P7C3 or vehicle. When mice were 3 months of age, they were sacrificed, and brain tissue was subjected to either Golgi-Cox staining or electrophysiological recording. As shown in Figure 4C, prolonged exposure to P7C3 repaired morphological deficits in dendritic branching of *npas3*^{-/-} dentate gyrus granular neurons. Moreover, as shown in Figure 4D, the electrophysiological deficit in the dentate gyrus of NPAS3-deficient mice was also corrected by this treatment. The corresponding electrophysiological deficit in the CA1 region of the hippocampus, however, was not affected (Figure 4D), underscoring the

specificity of P7C3 to improving function of the dentate gyrus in *npas3*^{-/-} mice. It was perplexing to observe that *npas3*^{-/-} mice having such poorly arborized dendritic branching displayed elevated fEPSP signatures. P7C3-induced enhancement of granular neuron arborization could foster restoration of either excitatory or inhibitory circuitry—or a combination of the two. The observed data favors restoration of inhibitory circuitry, yet further experimentation will be required to resolve this question.

To further investigate the impact of P7C3 on hippocampal circuitry, we used immunohistochemistry to visualize the expression levels of synapsin proteins 1 and 2. Synapsins are major phosphoproteins in synaptic vesicles that modulate neurotransmitter release. Immunohistochemical staining assays revealed P7C3-dependent normalization of synapsin 1 and 2 protein levels in the dentate gyrus molecular layer of *npas3*^{-/-} mice (Figure S3C). P7C3-mediated normalization was also observed for synaptobrevin 2, another marker of synaptic vesicle abundance (Figure S3D).

Relative to vehicle controls, prolonged P7C3 administration did not affect the health of mothers, embryos, weanlings, or young-adult mice. Gross histology of brain tissue was normal

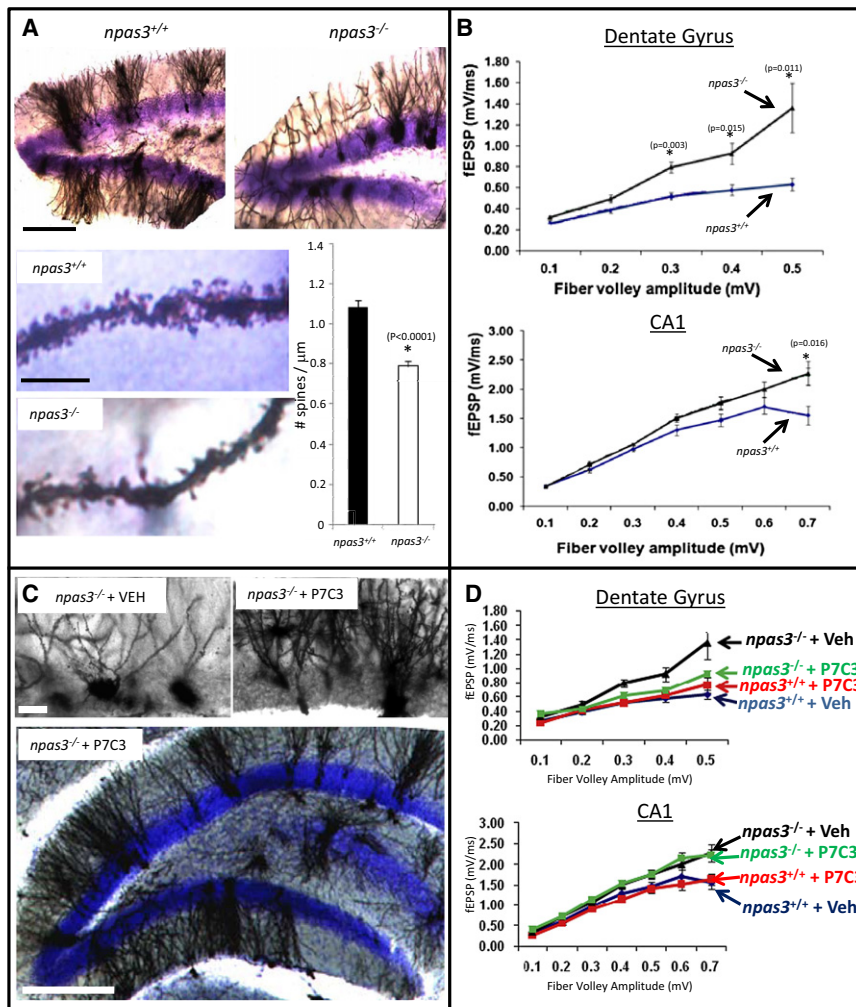


Figure 4. P7C3 Corrects Morphological and Electrophysiological Deficits in *npas3*^{-/-} Dentate Gyrus

(A) Golgi-Cox staining of the dentate gyrus revealed aberrant dendritic arborization in *npas3*^{-/-} mice relative to wild-type littermates (ten sections from each of five mice in each group). In addition to reduced dendritic length and branching, *npas3*^{-/-} dentate gyrus granular neurons also exhibited significantly reduced spine density relative to wild-type littermates ($p < 0.00001$, Student's *t* test). The top lower-power micrographs of dentate gyrus were taken at the same magnification (the scale bar represents 200 μm). For the bottom two higher-power micrographs of dendritic spines, the scale bar represents 10 μm .

(B) In hippocampal slice preparation from *npas3*^{-/-} mice, synaptic transmission, as assessed by whole-field recordings of fEPSPs, was increased both in the outer molecular layer of the dentate gyrus and the CA1 region of the hippocampus relative to that of wild-type mice.

(C) Golgi-Cox staining of dentate gyrus granular neurons showed that prolonged daily treatment of *npas3*^{-/-} mice with P7C3 enhanced dendritic arborization. Results shown are representative of ten sections from each of five mice in each group. Higher-power micrographs are shown on top (the scale bar represents 25 μm), and a lower-power micrograph illustrating the entire granular layer of the dentate gyrus is shown below (the scale bar represents 200 μm).

(D) Prolonged administration of P7C3 normalized whole field recordings of fEPSPs in the dentate gyrus but not the CA1 region of *npas3*^{-/-} mice. In all graphs, data are expressed as mean \pm SEM. See also Figure S3.

in both compound- and vehicle-treated animals, and there was no evidence of neuronal cell loss or degenerative changes (cytoplasmic eosinophilia, vacuolization, or nuclear pyknosis). The only morphological change, other than normalization of dendritic arborization of dentate gyrus granular neurons, was a compound-dependent increase in the thickness of the granular layer itself. The thickness of the granular layer of the dentate gyrus is roughly 40% less in *npas3*^{-/-} mice compared to wild-type littermates. Prolonged administration of P7C3 significantly corrected this deficit without affecting the thickness of other hippocampal layers in *npas3*^{-/-} mice (Figure S3E).

Recognizing that reduced thickness of the *npas3*^{-/-} dentate gyrus granular layer could be attributed to increased apoptosis of proliferating neural precursor cells, we examined the effect of P7C3 treatment on apoptosis in the hippocampus of *npas3*^{-/-} mice through immunohistochemical staining of CCSP3. After 12 days of orally delivered P7C3 (20 mg/kg) to adult *npas3*^{-/-} mice, a statistically significant reduction in CCSP3 staining was observed in the dentate gyrus (Figure 5). We thereby propose that P7C3 facilitates repair of the granular layer of the dentate gyrus in *npas3*^{-/-} mice by overcoming a genotype-specific enhancement in apoptosis.

P7C3 Protects Mitochondrial Membrane Integrity

Work pioneered by the laboratory of Xiaodong Wang has shown that an intrinsic pathway leading to apoptosis emanates from mitochondria (Liu et al., 1996; Yang et al., 1997). Knowing that P7C3 ameliorates the death of newborn neurons in the dentate gyrus in living mice, we wondered whether its function might relate to mitochondrial integrity. With the help of the Wang lab, assays were established to test whether P7C3 might protect cultured U2OS cells from calcium-induced mitochondrial dissolution (Distelmaier et al., 2008). Tetramethylrhodamine methyl ester (TMRM) dye is sequestered by active mitochondria, and, when loaded with TMRM, vehicle-treated cells released the dye within 15 min of exposure to the calcium ionophore A23187. By contrast, dye release was fully prevented in cells exposed to as little as 10nM of P7C3 (Figure 6). The P7C3A29 and P7C3A35 variants of P7C3 known to be inactive in vivo were also inactive in this assay. Preservation of mitochondrial membrane potential in this assay was observed for the *R*-enantiomer of P7C3-OMe, but not the *S*-enantiomer. Finally, protection of mitochondrial membrane permeability was observed at an enhanced level for the P7C3A20 variant, which also exhibited the highest level of proneurogenic activity (Figure 2). P7C3, but

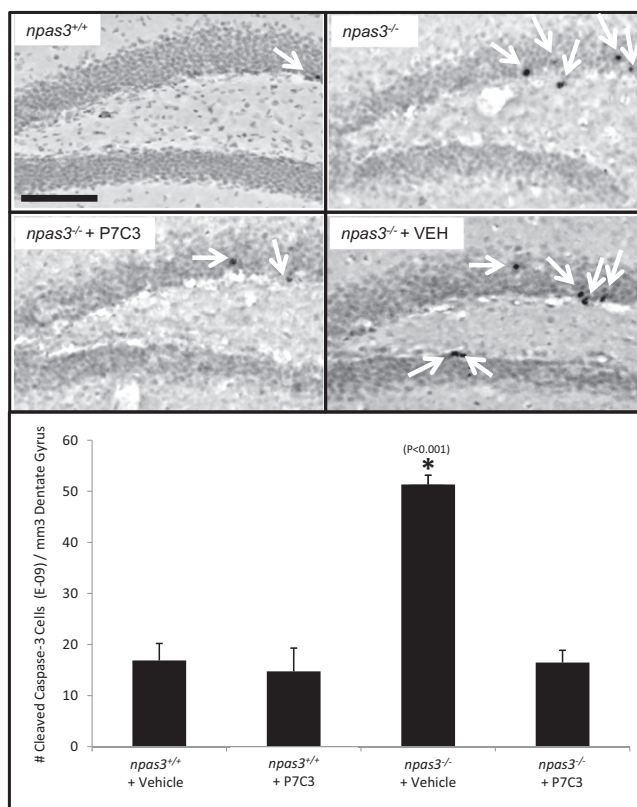


Figure 5. P7C3 Normalizes Elevated Levels of Hippocampal Apoptosis in *npas3*^{-/-} Mice

Immunohistochemical detection of CCSP3 showed elevated apoptosis in the dentate gyrus of *npas3*^{-/-} animals ($p < 0.001$). This was normalized by prolonged treatment with P7C3. Three adult animals were tested in each group. Data are expressed as mean \pm SEM. The scale bar represents 200 μ M.

not the inactive P7C3A29 derivative, was also capable of preserving mitochondrial integrity in cultured primary cortical neurons (Figure S4).

Comparison of P7C3 to Two Classes of Antiapoptotic Compounds

We next compared P7C3 to two other classes of putatively antiapoptotic compounds. Serono Pharmaceuticals Research Institute reported a series of brominated carbazole compounds capable of inhibiting Bid-mediated release of cytochrome *c* in isolated mitochondria (Bombrun et al., 2003). Independent studies from Russia also reported the discovery of a putatively antiapoptotic chemical. In the latter case a tetrahydro- γ -carboline, an antihistamine trade-named Dimebon, has been reported to block apoptosis of cortical neurons exposed to amyloid-beta peptide (Bachurin et al., 2001) and to protect mitochondrial membrane potential (Bachurin et al., 2003).

Chemical samples corresponding to the most active Serono compound (Figure 7, Serono compound 1), the least active Serono compound (Figure 7, Serono compound 2), and Dimebon (Figure 7) were obtained and tested for proneurogenic activity in mice. As shown in Figure 7A, the more active of the

Serono compounds exhibited proneurogenic activity superior to its less active relative. It was likewise observed that Dimebon was proneurogenic in vivo. Neither the active Serono compound nor Dimebon, however, reached an equivalent ceiling of proneurogenic efficacy as P7C3, and the dose required for maximal efficacy was higher in both cases than P7C3 (Figure 7A).

In an effort to quantitatively compare the in vivo, proneurogenic activities of P7C3, its A20 derivative, Dimebon, and the active Serono compound (Serono compound 1), we first sought to define the ceiling of efficacy (CoE) for each compound. The background level of neurogenesis in experiments conducted on wild-type mice throughout this study was consistently measured to be $14.5 \pm 1.1 \times 10^{-6}$ BrdU-positive neurons per mm^3 of the dentate gyrus (Figures 1 and 2 and Figure S1). Administration of P7C3 elevated the level to $30 \pm 1.4 \times 10^{-6}$ BrdU-positive neurons per mm^3 , corresponding to a 100% increase over basal levels (Figures 2 and 7 and Figure S1). The P7C3A20 variant increased the observed CoE level to 150% (Figure 2), whereas administration of both Dimebon and the active Serono compound achieved CoE values corresponding to a 60% increase in neurogenesis (Figure 7A).

To compare the relative potencies of the four chemicals, we asked what levels of drug administration were required to reach the 60% CoE level of Dimebon and Serono compound 1. As shown in Figure 7B, 30 μ M Dimebon, 10 μ M Serono compound 1, and between 1 and 3 μ M P7C3 were respectively required to reach the 60% CoE level. Moreover, as shown in Figure 2B, administration of only 0.1 μ M P7C3A20 variant exceeded the 60% CoE level. As judged by this simplistic definition of potency, the amount of P7C3 required to achieve the 60% CoE level was somewhere between one-tenth and one-thirtieth the level of Dimebon (1–3 μ M versus 30 μ M). Finally, the A20 derivative of P7C3 exceeded the CoE of Dimebon when administered at a dose of as little as 0.1 μ M, giving evidence of estimated potency 300 times that of Dimebon. Minimally, these interpretations suggest that further SAR assays should facilitate the generation of pharmacophores with substantial enhancement in potency and ceiling level of proneurogenic efficacy.

We next turned to the assay for calcium-induced mitochondrial dissolution to assess the activities of the two Serono compounds and Dimebon. As shown in Figure 7B, Dimebon protected mitochondrial membrane integrity at the 10 μ M and 1 μ M levels but not at submicromolar concentrations. Serono compound 1 also afforded protection of mitochondrial membrane potential, losing activity between the 100 nM and 10 nM test levels. Finally, Serono compound 2 was inactive at all doses tested. Not only do these data parallel the proneurogenic activities of the three compounds in living mice (Figure 7A), but—in the case of the two Serono compounds—parallel the reported activities in test tube reactions measuring protection of mitochondria from Bid-mediated cytochrome *c* release (Bombrun et al., 2003).

P7C3 Ameliorates Cognitive Decline in Aged Rats

If possible, we would have performed behavioral studies of learning and memory on *npas3*^{-/-} mice that had received prolonged treatment with either P7C3 or vehicle. Unfortunately, *npas3*^{-/-} mice are incapable of swimming and thus not able to

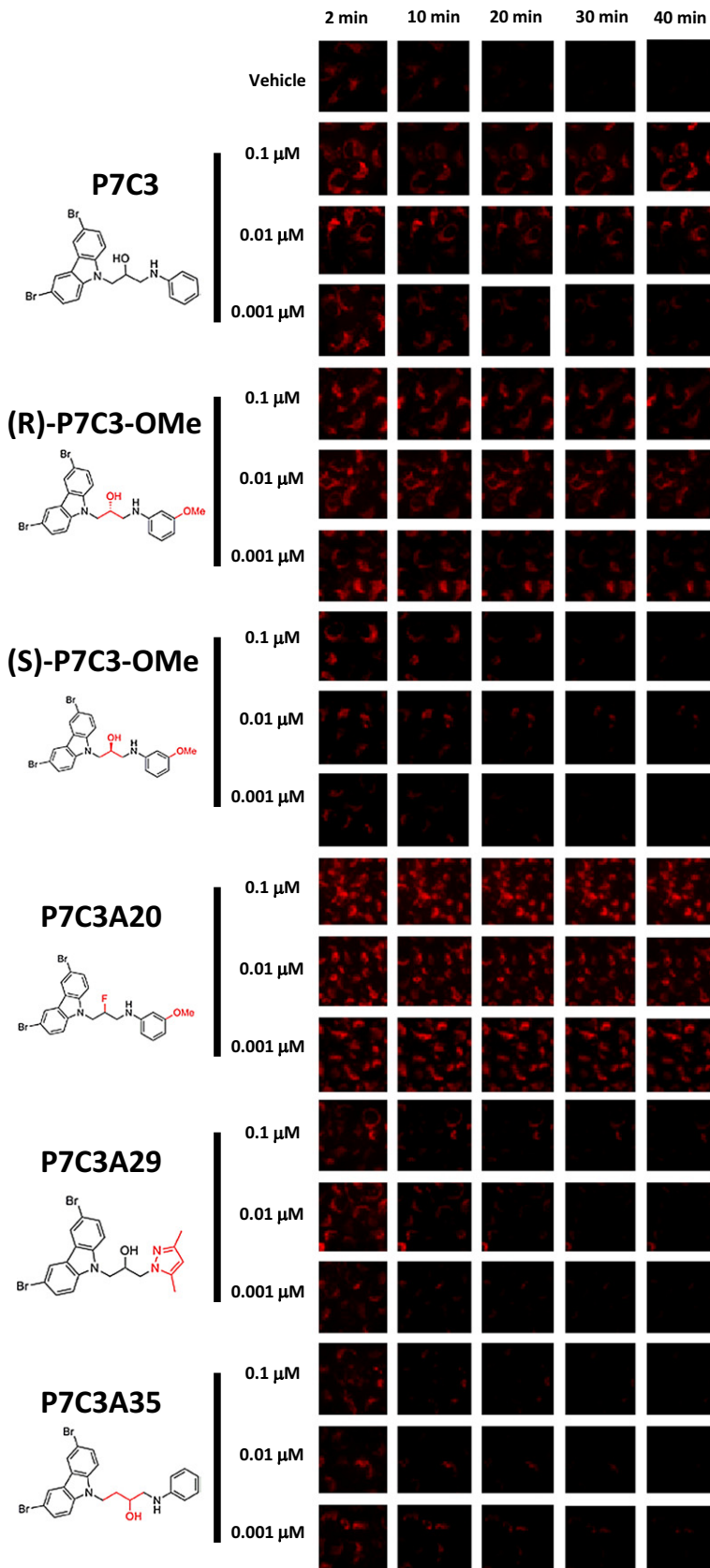


Figure 6. P7C3 and Its Analogs Preserve Mitochondrial Membrane Potential in Parallel to Proneurogenic Activity

U2OS cells were loaded with tetramethylrhodamine methyl ester (TMRM) dye and then exposed to the calcium ionophore A23187 either in the presence or absence of test compounds. P7C3 preserved mitochondrial membrane potential following exposure to the calcium ionophore A23187 in a dose-dependent manner. The protective effect of P7C3 was enantiomeric specific. The (*R*)-enantiomer of P7C3-OMe blocked dye release at levels as low as 1 nM, whereas the (*S*)-enantiomer failed to block dye release even at the highest drug dose tested (100 nM). The more active, proneurogenic analog (P7C3A20) exhibited dye release protection at all doses tested, yet analogs devoid of proneurogenic activity (P7C3A29 and P7C3A35) failed to preserve mitochondrial membrane potential at any test dose. Each compound was evaluated in triplicate with similar results. See also Figure S4.

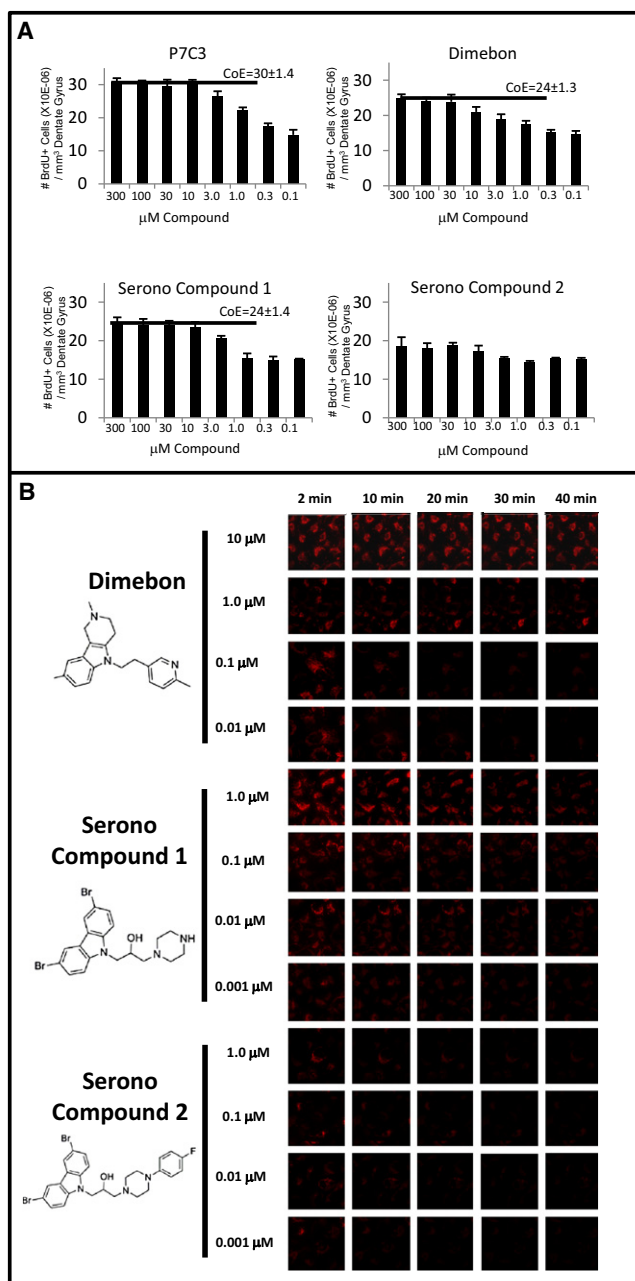


Figure 7. Comparison of P7C3 to Other Putative Antiapoptotic Agents

(A) Adult mice ($n = 4$ for each group) were administered equivalent dose escalations of P7C3, Dimebon, and Serono compounds 1 and 2 for 1 week. Dimebon was observed to enhance hippocampal neurogenesis, yet with diminished potency and efficacy relative to P7C3. Serono compound 1, which was more active than Serono compound 2 in inhibiting BID-mediated cytochrome *c* release from isolated mitochondria (Bombrun et al., 2003), was similarly superior to Serono compound 2 in enhancing *in vivo* neurogenesis. The proneurogenic efficacy of Serono compound 1 was comparable to Dimebon and diminished relative to P7C3. Horizontal bars designate ceiling of efficacy (CoE) levels for each compound. There is no CoE determination for Serono compound 2 because this agent did not significantly enhance neurogenesis. Data are expressed as mean \pm SEM.

be evaluated in the standard assay for hippocampus-dependent learning—the Morris water maze test. As such, we turned to aged Fisher rats as a means of performing behavioral tests capable of assessing the potential benefits of P7C3 on hippocampus-dependent learning. It is well established that normal rodent aging is associated with attenuation of hippocampal neurogenesis (Kuhn et al., 1996; Driscoll et al., 2006). Reduced neurogenesis in aged rats is likely related to increased neuronal apoptosis in the aged rat brain (Martin et al., 2002; Kim et al., 2010). These changes have been hypothesized to contribute to cognitive decline as a function of terminal aging.

We first evaluated whether P7C3 would enhance hippocampal neurogenesis in aged rats as it does in adult mice. Rats were injected with a daily, IP dose of either 10 mg/kg of P7C3 or vehicle, coincjected with a daily dose of BrdU, and then sacrificed after 7 days for immunohistochemistry. As shown in Figure S5A, compound-treated animals revealed a 500% increase in BrdU labeling in the dentate gyrus relative to vehicle-treated controls. Immunohistochemical staining with antibodies to doublecortin likewise revealed a robust, compound-specific enrichment in this marker of newborn neurons.

Having observed proneurogenic efficacy of P7C3 in this short-term assay, we then tested whether prolonged administration of P7C3 might ameliorate age-related decline in cognition by subjecting 18-month-old rats to daily administration of either 10 mg/kg of P7C3 or vehicle for 2 months. Animals of both groups were further subjected to weekly IP administration of BrdU (50 mg/kg) for later immunohistochemical measurements of hippocampal neurogenesis. As a control, both P7C3- and vehicle-treated groups were confirmed to display equal ability to physically participate in the task, and learn the task, as shown by decreased latency times to find the hidden platform over the 5 day training period, both before and after 2 months of treatment (Figure S5B). Moreover, neither swim speed (Figure S5C) nor locomotor activity (Figure S5D) varied with age or treatment paradigm.

After 2 months of compound or vehicle administration, cognitive ability was assessed blind to treatment group by removing the goal platform. Animals of the P7C3-treated group retained a statistically significant improvement in ability to navigate to the region of the missing platform, as evidenced by performance in the probe test. As shown in Figure 8A, when the platform was removed from the maze, rats treated with P7C3 crossed the precise location previously containing the platform significantly more often than vehicle-treated rats. Furthermore, P7C3-treated rats spent a higher percentage of time in the general goal area, defined as the quadrant previously containing the platform, than vehicle-treated rats ($35.5\% \pm 2.2\%$ for P7C3 treated, $28.1\% \pm 2.6\%$ for vehicle treated, Student's *t* Test, $p < 0.02$).

(B) Cultured U2OS cells were loaded with TMRM dye and exposed to a calcium ionophore in the presence of different doses of Dimebon, Serono compound 1, or Serono compound 2. Dimebon protected the mitochondrial membrane potential of U2OS cells only at the relatively high doses of 10 and 1 μ M. The more active, proneurogenic Serono compound 1 showed an enhanced ability to preserve mitochondrial membrane potential relative to the less active Serono compound 2. Serono compound 1 lost activity between 10 and 1 nM doses.

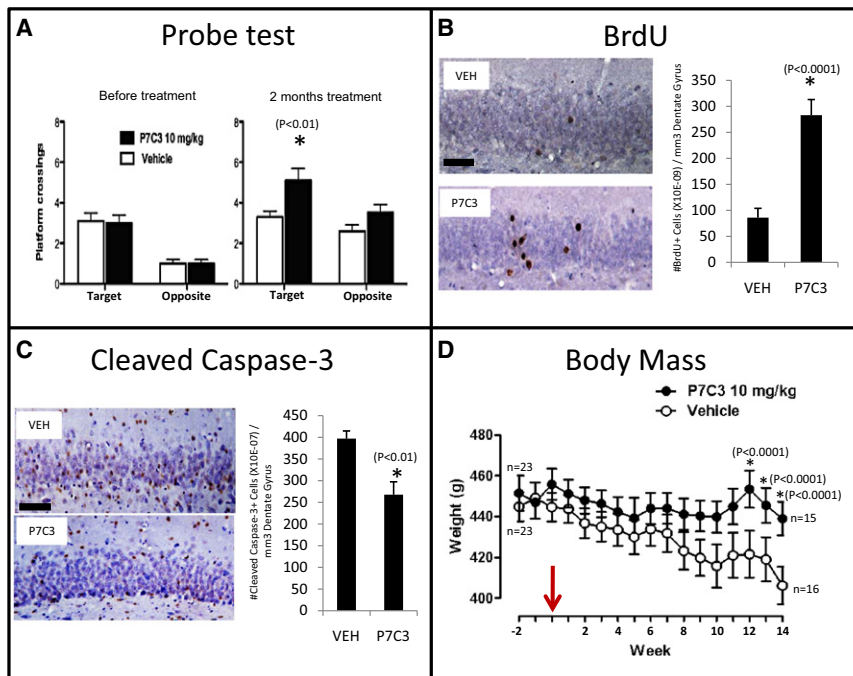


Figure 8. P7C3 Enhances Hippocampal Neurogenesis, Ameliorates Cognitive Decline, and Prevents Weight Loss in Terminally Aged Rats

(A) Prior to treatment, both groups ($n = 23$ for each group) showed similar frequency of crossings through the goal platform. After 2 months of treatment, however, P7C3-treated rats displayed a statistically significant increase of crossings through the goal platform area relative to vehicle-treated rats.

(B) P7C3-treated rats displayed significantly enhanced hippocampal neurogenesis, as assessed by BrdU incorporation, relative to vehicle-treated rats. Many more of the BrdU-labeled cells were noted to have migrated into the granular layer in P7C3-treated rats in comparison to vehicle-treated animals, consistent with their functional incorporation into the dentate gyrus as properly wired neurons. The scale bar represents $50 \mu\text{M}$.

(C) Relative to vehicle-treated animals, P7C3-treated rats displayed a significantly lower number of cleaved caspase 3-positive cells in the dentate gyrus, indicating that P7C3 was capable of inhibiting apoptosis in the aged rat brain. The scale bar represents $50 \mu\text{M}$.

(D) Relative to vehicle-treated animals, P7C3-treated rats were observed to maintain stable body weight as a function of terminal aging.

In all graphs data are expressed as mean \pm SEM. See also Figure S5.

After behavioral testing, animals were sacrificed for immunohistochemical detection of BrdU and CCSP3. As shown in Figure 8B, the dentate gyrus of rats exposed to P7C3 showed a 3-fold higher level of BrdU-positive neurons than that of the vehicle group. Moreover, P7C3-treated animals showed a statistically significant reduction in the number of CCSP3-positive cells relative to vehicle controls (Figure 8C).

Unexpectedly, administration of P7C3 helped rats maintain stable body weight with aging, in contrast to vehicle-treated rats, whose weight declined steadily with age (Figure 8D). P7C3-mediated effects on body weight were independent of food intake (Figure S5E), and treatment of aged rats with P7C3 had no effect on postfasting blood glucose levels (Figure S5E). It will be of interest to determine whether P7C3-mediated preservation of body weight in aged rats operates via central or peripheral modes of action.

DISCUSSION

We hereby provide evidence for the discovery of a series of proneurogenic, neuroprotective compounds. The aminopropyl carbazole designated P7C3 was one of eight proneurogenic compounds discovered in an unbiased screen of 1000 drug-like chemicals. P7C3 is orally bioavailable, endowed with a relatively long half-life, capable of crossing the blood-brain barrier, and safely tolerated by mice exposed to the chemical throughout late embryonic development, early postnatal development, and the first 2 months after weaning. P7C3 protects the survival of newborn neurons in the dentate gyrus, the majority of which normally die as they transit an arduous “differentiation gauntlet”

lasting upwards of 1 month before surviving cells become functionally wired into the central nervous system. Administration of P7C3 to normal mice, as well as *npas3*^{-/-} mice, enhanced survival of neurons subsequent to their birth in the SGZ. Compound administration promoted the generation of mature granular neurons that appeared to be normal by morphological and electrophysiological criteria. Finally, prolonged administration of P7C3 to aged rats ameliorated age-related decline in cognition. We hypothesize that this behavioral enhancement in cognition may be due to P7C3-mediated improvement in the survival of newborn hippocampal neurons.

When exposed to a calcium ionophore, the mitochondria of cultured cells lose membrane potential and release a readily detectible vital dye. Treatment of cultured cells with low nanomolar concentrations of P7C3 blocked mitochondrial dissolution in response to increased levels of intracellular calcium. Inactive variants of P7C3, as assayed in living mice, were inactive in this assay of mitochondrial membrane permeability protection. It was likewise observed that the single SAR variant of P7C3 with enhanced potency and efficacy in the *in vivo* assay of neurogenesis also showed superior activity in the mitochondrial assay. Finally, the active, *R*-enantiomer of P7C3 was observed to be active in the mitochondrial assay—but not the *S*-enantiomer. We tentatively conclude that the *in vivo*, proneurogenic activity of P7C3 can be attributed to its capacity to protect mitochondrial integrity and thereby mitigate the death of newborn neurons between their time of birth and functional incorporation into the granular layer of the dentate gyrus. The validity of this conclusion will await identification of the molecular target of the compound.

Mice tailored to either eliminate expression of the proapoptotic Bax protein (Sun et al., 2004; Kim et al., 2009) or overexpress the antiapoptotic Bcl-2 protein (Kuhn et al., 2005) have been shown to over-produce newborn neurons in the dentate gyrus of the adult brain by manipulating apoptosis. We tentatively conclude that P7C3 achieves a similar functional outcome as genetic manipulation of the pro- and antiapoptotic Bax and Bcl2 proteins. This interpretation, in retrospect, may explain why P7C3 was observed to enhance BrdU incorporation selectively in the dentate gyrus of the adult mouse brain. If the compound only functions to enhance the survival of newborn neurons, and has no role in stimulating the birth of neurons, it would be expected to enhance BrdU incorporation only in brain regions endogenously active in neurogenesis.

Whereas we have not carefully monitored the effects of P7C3 in all regions of the rodent brain, the only other brain region clearly and reproducibly observed to accumulate higher levels of BrdU-positive neurons in response to administration of P7C3 was the rostral migratory stream (RMS) (data not shown). The RMS contains migrating neurons born in the SVZ and destined for incorporation into the olfactory bulb. Further studies of the effects of P7C3 on SVZ-localized neurogenesis will be required in order to assess whether common mechanisms are shared with what are reported herein for P7C3-mediated effects on neurogenesis in the dentate gyrus.

If the efficacy of P7C3 can be attributed to its ability to protect newborn neurons from apoptosis, it is perplexing that prolonged administration of the compound throughout the third trimester of embryonic development, all of weaning, and 2 months after weaning—at doses considerably higher than that required for proneurogenic efficacy—did not result in significant aberration in mouse development. Apoptosis is vitally important for a myriad of developmental processes. As such, it would appear that the effects of P7C3 are somehow restricted to unique applications of apoptosis or that the survival of newborn neurons in the dentate gyrus is unusually sensitive to apoptosis.

Perhaps the most surprising discovery reported herein is the functional similarity between P7C3 and two other classes of antiapoptotic compounds (the Serono compounds and Dimebon), shown in our studies to be proneurogenic. Dimebon is a tetrahydro- γ -carboline long deployed in Russia as an antihistamine therapeutic. Anecdotal observations by Russian physicians raised the possibility that Dimebon might ameliorate the symptoms of age related cognitive decline (O'Brien, 2008; Burns and Jacoby, 2008), prompting an American biotechnology company to perform Food and Drug Administration-sanctioned clinical trials on patients suffering from various forms of neurodegenerative disease. As reported in the *Lancet* in 2008, prolonged treatment of Alzheimer's patients with Dimebon substantially improved symptoms (Doody et al., 2008). Disconcertingly, unpublished reports coming from a larger, phase 3 clinical trial failed to provide evidence of any difference in disease progression between Dimebon- and placebo-treated patients (Miller, 2010).

The results of this study raise the possibility that Dimebon, P7C3, and the Serono compounds may operate via a common mechanistic pathway. If correct, this conclusion almost certainly rules out the possibility that the clinical utility of Dimebon as

a therapeutic treatment for age-related decline in cognition can be attributed to its antihistamine activity. Highly effective proneurogenic derivatives of P7C3 have been found to retain no detectable inhibitory activity to any of the known histamine receptors (McKnight et al., 2010, patent pending). The speculative idea that these chemicals share a common mode of action will only be rigorously tested upon identification of their molecular target(s). For the sake of patients suffering from Alzheimer's disease, it is hoped that the apparently marginal clinical utility of Dimebon might be enhanced by improvements in both its potency and ceiling of proneurogenic, neuroprotective efficacy. If so, our work offers concrete assays for the development of improved versions of these neuroprotective drugs.

EXPERIMENTAL PROCEDURES

Approval for the animal experiments described herein was obtained by the University of Texas Southwestern Medical Center Institutional Animal Care and Use Committee. [Extended Experimental Procedures](#) are available online.

Immunohistochemistry

Standard procedures were employed for staining paraformaldehyde-perfused brain tissue with the antibodies against the following antigens: BrdU (1:100, Roche), CCSP3 (1:200, Cell Signaling), synapsin 1/2 (1:250, Synaptic Systems), synaptobrevin 2 (1:500, Synaptic Systems), Prox1 (1:1000, Chemicon), NeuN (1:1000, Millipore), GFAP (1:2000, Millipore), S100 β (1:2000, Sigma), GSTpi (1:3000, BD Biosciences), and PDGF α (1:500, BD Pharmingen).

Statistics

All p values were obtained with the Student's t test.

Electrophysiology

Hippocampal slices were maintained at 30°C and perfused continuously with aCSF in the recording chamber. In the dentate gyrus, stimulating and recording electrodes were positioned in the outer molecular layer, which is innervated by axons of the perforant pathway from the entorhinal cortex. In CA1, stimulation and recording electrodes were positioned in the stratum radiatum, which is innervated by the Schaffer collateral axons from CA3. Stimulus intensity was increased in 5 μ A increments, the slope of the decreasing part of field potentials was measured, and fEPSP was quantified relative to the amplitude of the fiber volley, which represents firing of action potentials in presynaptic axons. For input-output measurements, stimulus intensity was increased in 5 μ A increments up to 100 μ A. FPs were filtered at 2 kHz, acquired, and digitized at 10 kHz on a computer with customized LabVIEW software (National Instruments, Austin, TX). The 20/80 slope of the FP was used in this experiment.

Golgi-Cox Staining

Golgi-Cox staining was accomplished with the rapid Golgi stain kit (FD Neuro-Technologies, PK-401). Tissue was analyzed with an Olympus BX51 microscope and NeuroLucida software (MBF Biotechnology).

Mitochondrial Dissolution Assay

Live-cell imaging of mitochondrial integrity was executed according to established methods (Distelmaier et al., 2008) in U2OS cells and primary cortical neurons from E17 rats.

SUPPLEMENTAL INFORMATION

Supplemental Information includes Extended Experimental Procedures, five figures, one table, and chemical synthesis and can be found with this article online at [doi:10.1016/j.cell.2010.06.018](https://doi.org/10.1016/j.cell.2010.06.018).

ACKNOWLEDGMENTS

We thank the Wang lab for extensive help in establishing the live-cell imaging assay used to measure mitochondrial membrane permeability; Xiaodong Wang and Sol Snyder for invaluable scientific input; Patrick Harran for helping select the 1000 chemicals chosen for in vivo screening; David Russell and members of the Russell lab for extensive help in electrophysiological recording assays; Christopher Cowan and members of the Cowan laboratory for assistance with primary neuronal cultures; Farah Veerjee, Saira Hussein, Latisha McDaniel, Ruth Starwalt, and Leeju Wu for technical assistance; and Huda Zoghbi, Sol Snyder, Joe Goldstein, Ueli Schibler, Al Gilman, Mike Brown, Richard Axel, and Martin Raff for critical review of the manuscript. We thank Angela Diehl for help with the graphical abstract artwork. This work was supported by grants from The Hartwell Foundation, Staglin Family fund, University of Texas Southwestern Medical Center High Risk/High Impact research fund, National Alliance for Research on Schizophrenia and Depression, and Morton H. Meyerson Family Tzedakah Fund awarded to A.A.P.; a Transformative RO1 grant (National Institute of Mental Health [NIMH] 1R01MH087986) awarded to A.A.P. and S.L.M.; and a National Institutes of Health (NIH) Pioneer grant (National Institute of General Medical Sciences 5DP1OD000276), a NIH Method to Extend Research in Time grant (NIMH RO1MH59388), a National Cancer Institute Program Project Grant (5PO1CA95471), a Simons Foundation Autism Research Initiative grant from the Simons Foundation, and funds from an anonymous donor provided to S.L.M.

Received: April 25, 2010

Revised: June 4, 2010

Accepted: June 10, 2010

Published: July 8, 2010

REFERENCES

- Altman, J. (1962). Are new neurons formed in the brains of adult mammals? *Science* 135, 1127–1128.
- Altman, J., and Das, G.D. (1965). Autoradiographic and histological evidence of postnatal hippocampal neurogenesis in rats. *J. Comp. Neurol.* 124, 319–335.
- Bachurin, S., Bukatina, E., Lermontova, N., Tkachenko, S., Afanasiev, A., Grigoriev, V., Grigorjeva, I., Ivanov, Y., Sablin, S., and Zefirov, N. (2001). Antihistamine agent Dimebon as a novel neuroprotector and a cognition enhancer. *Ann. N Y Acad. Sci.* 939, 425–435.
- Bachurin, S.O., Shevtsova, E.P., Kireeva, E.G., Oxenkrug, G.F., and Sablin, S.O. (2003). Mitochondria as a target for neurotoxins and neuroprotective agents. *Ann. N Y Acad. Sci.* 993, 334–344, discussion 345–349.
- Boldrini, M., Underwood, M.D., Hen, R., Rosoklijja, G.B., Dwork, A.J., John Mann, J., and Arango, V. (2009). Antidepressants increase neural progenitor cells in the human hippocampus. *Neuropsychopharmacology* 34, 2376–2389.
- Bombrun, A., Gerber, P., Casi, G., Terradillos, O., Antonsson, B., and Halazy, S. (2003). 3,6-dibromocarbazole piperazine derivatives of 2-propranolol as first inhibitors of cytochrome c release via Bax channel modulation. *J. Med. Chem.* 46, 4365–4368.
- Brown, J.P., Couillard-Després, S., Cooper-Kuhn, C.M., Winkler, J., Aigner, L., and Kuhn, H.G. (2003). Transient expression of doublecortin during adult neurogenesis. *J. Comp. Neurol.* 467, 1–10.
- Burns, A., and Jacoby, R. (2008). Dimebon in Alzheimer's disease: old drug for new indication. *Lancet* 372, 179–180.
- Distelmaier, F., Koopman, W.J., Testa, E.R., de Jong, A.S., Swarts, H.G., Mayatepek, E., Smeitink, J.A., and Willems, P.H. (2008). Life cell quantification of mitochondrial membrane potential at the single organelle level. *Cytometry A* 73, 129–138.
- Doody, R.S., Gavrilova, S.I., Sano, M., Thomas, R.G., Aisen, P.S., Bachurin, S.O., Seely, L., and Hung, D.; dimebon investigators. (2008). Effect of dimebon on cognition, activities of daily living, behaviour, and global function in patients with mild-to-moderate Alzheimer's disease: a randomised, double-blind, placebo-controlled study. *Lancet* 372, 207–215.
- Driscoll, I., Howard, S.R., Stone, J.C., Monfils, M.H., Tomanek, B., Brooks, W.M., and Sutherland, R.J. (2006). The aging hippocampus: a multi-level analysis in the rat. *Neuroscience* 139, 1173–1185.
- Erbel-Sieler, C., Dudley, C., Zhou, Y., Wu, X., Estill, S.J., Han, T., Diaz-Arrastia, R., Brunskill, E.W., Potter, S.S., and McKnight, S.L. (2004). Behavioral and regulatory abnormalities in mice deficient in the NPAS1 and NPAS3 transcription factors. *Proc. Natl. Acad. Sci. USA* 101, 13648–13653.
- Gross, C.G. (2000). Neurogenesis in the adult brain: death of a dogma. *Natl. Rev.* 1, 67–72.
- Kamnasaran, D., Muir, W.J., Ferguson-Smith, M.A., and Cox, D.W. (2003). Disruption of the neuronal PAS3 gene in a family affected with schizophrenia. *J. Med. Genet.* 40, 325–332.
- Kempermann, G., Kuhn, H.G., and Gage, F.H. (1997). More hippocampal neurons in adult mice living in an enriched environment. *Nature* 386, 493–495.
- Kim, W.R., Park, O.H., Choi, S., Choi, S.Y., Park, S.K., Lee, K.J., Rhyu, I.J., Kim, H., Lee, Y.K., Kim, H.T., et al. (2009). The maintenance of specific aspects of neuronal function and behavior is dependent on programmed cell death of adult-generated neurons in the dentate gyrus. *Eur. J. Neurosci.* 29, 1408–1421.
- Kim, S.E., Ko, I.G., Kim, B.K., Shin, M.S., Cho, S., Kim, C.J., Kim, S.H., Baek, S.S., Lee, E.K., and Jee, Y.S. (2010). Treadmill exercise prevents aging-induced failure of memory through an increase in neurogenesis and suppression of apoptosis in rat hippocampus. *Exp. Gerontol.* 45, 357–365.
- Kuhn, H.G., Dickinson-Anson, H., and Gage, F.H. (1996). Neurogenesis in the dentate gyrus of the adult rat: age-related decrease of neuronal progenitor proliferation. *J. Neurosci.* 16, 2027–2033.
- Kuhn, H.G., Biebl, M., Wilhelm, D., Li, M., Friedlander, R.M., and Winkler, J. (2005). Increased generation of granule cells in adult Bcl-2-overexpressing mice: a role for cell death during continued hippocampal neurogenesis. *Eur. J. Neurosci.* 22, 1907–1915.
- Liu, X., Kim, C.N., Yang, J., Jemmerson, R., and Wang, X. (1996). Induction of apoptotic program in cell-free extracts: requirement for dATP and cytochrome c. *Cell* 86, 147–157.
- Macintyre, G., Alford, T., Xiong, L., Rouleau, G.A., Tibbo, P.G., and Cox, D.W. (2010). Association of NPAS3 exonic variation with schizophrenia. *Schizophr. Res.*, in press. Published online May 11, 2010. 10.1016/j.schres.2010.04.002.
- Martin, D.S., Lonergan, P.E., Boland, B., Fogarty, M.P., Brady, M., Horrobin, D.F., Campbell, V.A., and Lynch, M.A. (2002). Apoptotic changes in the aged brain are triggered by interleukin-1 β -induced activation of p38 and reversed by treatment with eicosapentaenoic acid. *J. Biol. Chem.* 277, 34239–34246.
- McKnight, S.L., Pieper, A.A., Ready, J.M., DeBrabander, J. July 2010. Pro-neurogenic compounds. U.S. patent 2010/020681.
- Miller, G. (2010). Pharmacology. The puzzling rise and fall of a dark-horse Alzheimer's drug. *Science* 327, 1309.
- O'Brien, J.T. (2008). A promising new treatment for Alzheimer's disease? *Lancet Neurol.* 7, 768–769.
- Paton, J.A., and Nottebohm, F.N. (1984). Neurons generated in the adult brain are recruited into functional circuits. *Science* 225, 1046–1048.
- Pickard, B.S., Malloy, M.P., Porteous, D.J., Blackwood, D.H., and Muir, W.J. (2005). Disruption of a brain transcription factor, NPAS3, is associated with schizophrenia and learning disability. *Am. J. Med. Genet. B. Neuropsychiatr. Genet.* 136B, 26–32.
- Pickard, B.S., Pieper, A.A., Porteous, D.J., Blackwood, D.H., and Muir, W.J. (2006). The NPAS3 gene—emerging evidence for a role in psychiatric illness. *Ann. Med.* 38, 439–448.
- Pickard, B.S., Christoforou, A., Thomson, P.A., Fawkes, A., Evans, K.L., Morris, S.W., Porteous, D.J., Blackwood, D.H., and Muir, W.J. (2009). Interacting haplotypes at the NPAS3 locus alter risk of schizophrenia and bipolar disorder. *Mol. Psychiatry* 14, 874–884.
- Pieper, A.A., Wu, X., Han, T.W., Estill, S.J., Dang, Q., Wu, L.C., Reece-Finannon, S., Dudley, C.A., Richardson, J.A., Brat, D.J., and McKnight, S.L. (2005). The neuronal PAS domain protein 3 transcription factor controls

FGF-mediated adult hippocampal neurogenesis in mice. *Proc. Natl. Acad. Sci. USA* 102, 14052–14057.

Schmidt, H.D., and Duman, R.S. (2007). The role of neurotrophic factors in adult hippocampal neurogenesis, antidepressant treatments and animal models of depressive-like behavior. *Behav. Pharmacol.* 18, 391–418.

Stanfield, B.B., and Cowan, W.M. (1988). The development of the hippocampal region. In *Cerebral Cortex*, E.G. Jones and A. Peters, eds. (New York: Plenum Press), pp. 91–131.

Sun, W., Winseck, A., Vinsant, S., Park, O.H., Kim, H., and Oppenheim, R.W. (2004). Programmed cell death of adult-generated hippocampal neurons is mediated by the proapoptotic gene Bax. *J. Neurosci.* 24, 11205–11213.

van Praag, H., Kempermann, G., and Gage, F.H. (1999). Running increases cell proliferation and neurogenesis in the adult mouse dentate gyrus. *Nat. Neurosci.* 2, 266–270.

Yang, J., Liu, X., Bhalla, K., Kim, C.N., Ibrado, A.M., Cai, J., Peng, T.I., Jones, D.P., and Wang, X. (1997). Prevention of apoptosis by Bcl-2: release of cytochrome c from mitochondria blocked. *Science* 275, 1129–1132.